Please cite this paper as

Cai Q and Zhu S (2020) A Unified Strategy for Overall Impedance Optimization in Vibration-based Electromagnetic Energy Harvester. International Journal of Mechanical Sciences. 165: 105198. https://doi.org/10.1016/j.ijmecsci.2019.105198

A Unified Strategy for Overall Impedance Optimization in Vibration-based Electromagnetic Energy Harvester

Qin-lin CAI[1] and Songye ZHU*[,1,2]

1. Department of Civil and Environmental Engineering, The Hong Kong Polytechnic University, Kowloon, Hong Kong, China

2. The Hong Kong Branch of National Rail Transit Electrification and Automation Engineering Technology Research Center, The Hong Kong Polytechnic University, Kowloon, Hong Kong, China

* Corresponding author: Dr. Songye Zhu, songye.zhu@polyu.edu.hk

Abstract

Vibration-based electromagnetic energy harvesters involves the apparent coupling effect between the dynamics of mechanical structures and electric circuit. Such a coupling effect complicates the optimization of energy harvesting circuit impedance in the design of energy harvesters. The classical impedance matching that ignores the coupling effect becomes inapplicable. This paper proposes an unified overall impedance optimization strategy for the optimization of circuit load impedance to achieve the maximum output power and power efficiency. By converting the mechanical structures of single-degree-of-freedom (SDOF) and multiple-degree-of-freedom (MDOF) energy harvesters into equivalent circuit models, the electro-mechanical coupling is simplified as the coupling effect insider an electric circuit. This conversion provides the insight into an overall impedance optimization framework from the pure electric circuit perspective. Different optimal impedance values of energy harvesting circuits under different excitation types (harmonic and random) were derived within the proposed overall impedance optimization framework. The optimal impedance values for the maximum output power depend on the circuit dynamics, structural characteristics, and excitation types; while the optimal impedance values for the maximum power efficiency is related to the inherent damping of the structure and transducer, but independent with excitation types. Numerical simulations of various cases were conducted, including resonant, non-resonant and random excitation in SDOF and MDOF harvester. The simulation results successfully validate the effectiveness and accuracy of the proposed overall impedance optimization strategy for enhancing the energy performance of vibration-based electromagnetic energy harvesters.

Keywords: impedance matching, vibration-based electromagnetic energy harvesting, equivalent circuit model, power optimization, coupling effect

Nomenclature

L_s	Inductor of the power source	P_{out}	Output power of the harvester
L_{coil}	Internal inductor of the electromagnetic motor	P_{in}	Input power of the harvester
L_{str}	Equivalent structural inductor of the SDOF harvester	η	Power efficiency of the harvester
L_{str_i}	ith equivalent structural inductor of the MDOF harvester	η_1	Conversion efficiency from the mechanical power to electromagnetic
R_s	Resistor of the power source	η_2	Conversion efficiency from the total electrical power to harvesting circuit
R_{coil}	Internal resistor of the electromagnetic motor	η_3	Conversion efficiency of the harvesting circuit, equals to 1 in this study
R_{str}	Equivalent structural resistor of SDOF harvester	i_s	Current of the current source
R_{str_i}	ith equivalent structural resistor of the MDOF harvester	m_{str}	Mass of the SDOF harvester
R_{load}	Loading resistor of the harvesting circuit	m_{str_i}	Mass of the ith degree of freedom in MDOF harvester
R_{p+str}	Equivalent resistor of the SDOF harvester's and parasitic damping	c_{str}	Inherent damping coefficient of the SDOF harvester
R_p	Equivalent resistor of parasitic damping	c_{str_i}	Inherent damping coefficient of the ith degree of freedom in MDOF harvester
R_{Th}	Thévenin equivalent resistance	c_p	Parasitic damping of the electromagnetic motor
C_s	Capacitor of the power source	k_{str}	Stiffness of SDOF harvester
C_{str}	Equivalent capacitor of the primary structure mass	k_{str_i}	Stiffness of the ith degree of freedom in MDOF harvester
C_{str_i}	ith equivalent structural capacitor of the MDOF harvester	K_{eq}	Machine constant of the electromagnetic motor
χ_{load}	Loading reactance of the harvesting circuit	θ	Phase angle between the current and voltage in harvesting circuit
χ_{Th}	Thévenin equivalent reactance	S_I	Average power spectral density of the random current source
Z_{out}	Impedance of the harvesting circuit	S_o	Average power spectral density of the random input
Z_{Tol}	Impedance of the harvesting circuit and transducer	f_{res}	Frequency of excitation
Z_{Th}	Thévenin equivalent impedance	f_{res_i}	ith order resonant frequency in MDOF harvester
V_{Th}	Thévenin equivalent voltage	$\dot{x}$	Relative velocity between two terminals
V_s	Voltage of the voltage source		

1. Introduction

Energy harvesting is known as the process of extracting energy from surrounding environments and converting into usable energy (Park et al. 2008). Vibration-based energy harvesting, as a down-to-earth renewable energy source, has evoked immerse research interest, because of its wide availability and suitability in many situations. The harvested energy can theoretically provide a sustainable power source to low-power wireless sensors, thus solving the power supply problems associated with wireless sensors (Shen et al. 2012; Sazonov et al. 2009; Cahill et al. 2014; Iqbal and Khan, 2018). However, the output power of many energy harvesting devices usually ranges from μWs to mWs (Mitcheson, 2005), whereas the typical power consumption of a wireless sensor is from tens to hundreds of mWs (Priya, 2005). Therefore, great efforts have been made recently to optimize the design of vibration-based energy harvesters, from either mechanical or electrical perspectives (Saha et al. 2006; Kong et al. 2010; Challa et al. 2011; Yang et al. 2009; Tang et al. 2010; Zhao et al. 2018; Liao and Sodano, 2018; Liu et al. 2018).

Different transduction mechanisms including piezoelectric, electromagnetic and electrostatic have been explored to convert vibration energy into electrical energy (Erturk, 2009). The optimization of electromagnetic energy harvesting devices has been more frequently studied, considering its relatively higher output power (at least mW level) compared with other types of small-scale harvesters (Shen, 2014). For energy harvesting circuits, the traditional impedance matching (IM) has been applied to meet the maximum output power condition (Kasyap et al. 2002; Hambley, 2008). Zhu et al. (2012) presented a theoretical and experimental study of the linear electromagnetic motor connected with four representative circuits when excited by a constant harmonic load. The conditions for maximum output power and maximum efficiency were derived separately, and the corresponding result was consistent with the IM strategy. The constant input signal in their derivations assumes that the variation of the energy harvesting circuits does not influence the input signal, which may not be true in the practical applications when the circuit inevitably affects the dynamics of vibration-based energy harvesters and changes the input signal. In fact, the resistance, inductance and capacitance in the external circuit could be regarded as analogues to damping, stiffness and inertance, respectively, added to the primary structure (Firestone, 1993; Zhu et al. 2013; Li and Zhu, 2018). Ye et al. (2017) conducted the power analysis of a single-degree-of-freedom (SDOF) vibration-based energy harvester and showed that the generated output power was greatly affected by the excitation frequency and electromagnetic damping and stiffness. These parameters influence both the structural dynamics of the SDOF harvesters and the efficiency of the energy harvesting

circuit, and thus such effects should be taken into consideration simultaneously to maximize the output power.

Williams and Yates (2001) reached the essentially conclusion that the maximum output power of an SDOF harvester corresponds to the following two conditions: (1) the excitation frequency is equal to the natural frequency of the energy harvester, which generates the resonance of the harvester; (2) the electrical impedance of the load equals the equivalent impedance of the mechanical damping. By considering the coil characteristic of an electromagnetic harvester, Stephen (2006) reached a modified conclusion that the maximum out power in a resonance state could be achieved when the loading resistance of the circuit was equal to the sum of the coil resistance and the electrical analogue of the mechanical damping coefficient.

These aforementioned optimization in the literature mainly focused on the ideally resonant state. In a more general non-resonant situation, Cheng et al. (2007) determined the maximum power generation delivered into the electrical load through the complex conjugate of the source impedance, and proposed an overall impedance optimization with consideration of the primary structure characteristic under harmonic excitation. Cammarano et al. (2010) derived a similar optimal result and tried to re-tune a resonant state of the energy harvester through this theory. More recently, Cammarano et al. (2014) derived an optimum resistance for a nonlinear energy harvester for a fixed sinusoidal excitation considering the influence of the structure by ignoring the internal resistor and inductor of the coil. The analysis results indicated that the optimal resistance was related to several parameters, such as structural frequency, excitation frequency and mechanical damping.

Surprisingly, rare attention has been directed to the optimal conditions of vibration-based harvester under random excitations, an arguably more common types of environmental vibrations. Another apparent deficiency is that the majority of the previous optimization studies focused on SDOF harvesters, despite the fact that the harvesters may sometimes be multi-degree-of-freedom (MDOF) structures (e.g., Yang et al. 2009; Aldraihem and Baz, 2011; Magdy et al. 2014; Tang and Yang, 2012; Xiao et al. 2016). Hence, the optimizations presented in the previous studies only provide the incomplete answer to individual cases. This paper aims to propose a unified solution for vibration-based energy harvesters based on the overall impedance optimization strategy, which is applicable to either SDOF or MDOF energy harvesters under different excitations. The paper is organized as follows: after the introduction, the classical IM strategy is introduced first in Section 2. Then, based on the dynamic analogy between mechanical and electrical systems, the vibration-based electromagnetic energy

harvester is represented by an alternative equivalent circuit entirely in the electrical domain. With such an equivalent circuit model, the optimal conditions for output power and efficiency are derived mathematically under various excitation types in Section 3. Subsequently, numerical models are established to simulate six different scenarios (SDOF and MDOF harvesters under resonant, non-resonant and random excitations) and validate the proposed overall impedance optimization strategy in Section 4. Finally, the conclusion of this paper are drawn in Section 5.

2. Classical IM

2.1 Voltage Source

The traditional IM in electronics refers to the practice of designing the loading impedance to maximize the power transfer. Fig. 1 shows a representative electrical model with a voltage source V_s and internal impedance (Capacitance C_s, Inductance L_s and Resistance R_s). The corresponding source impedance Z_s is given as,

$$Z_s = R_s + \left(\omega L_s - \frac{1}{\omega C_s} \right) j \tag{1}$$

where ω is the frequency of the voltage source. To maximize the average power transfer to the load, the loading impedance Z_{load} should be the complex conjugate of the source impedance, which is commonly known as the classical IM,

$$Z_{load} = R_{load} + \chi_{load}\, j \tag{2}$$

where

$$R_{load} = \mathrm{Re}\left(Z_s \right) = R_s \tag{2.1}$$

$$\chi_{load} = -\mathrm{Im}\left(Z_s \right) = \frac{1}{\omega C_s} - \omega L_s \tag{2.2}$$

where $\mathrm{Re}(\cdot)$ and $\mathrm{Im}(\cdot)$ denote the real and imaginary parts of the concerned impedance, and R_{load} and χ_{load} are the loading resistant and reactance, respectively.

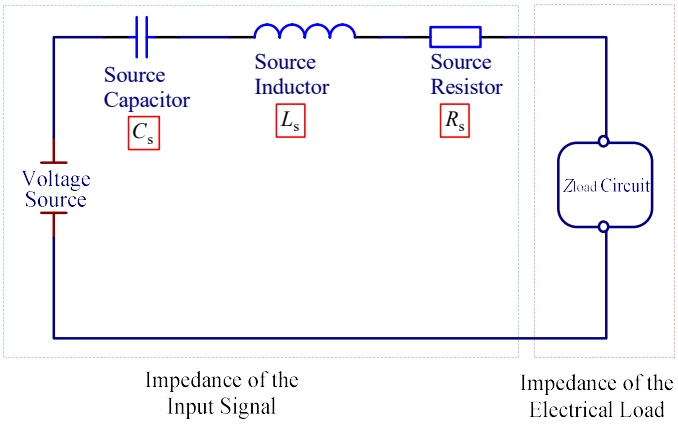

Fig. 1 Classical IM with voltage source

2.2 Current Source

For a circuit with a current source or more complex electric network, the Thévenin's theorem presents a standard technique to convert a complex circuit into an equivalent simplified circuit with a voltage source in a series connection with an internal impedance,

- *The Thévenin equivalent voltage V_{Th} is the open circuit voltage at the output terminals of the original circuit;*
- *The Thévenin equivalent impedance Z_{Th} can be calculated across the terminals using the formulae for series and parallel circuits after replacing the current and voltage sources with open and short circuits, respectively.*

Fig. 2 shows a classical electrical circuit with a current source. The corresponding Thévenin parameters are,

$$V_{\mathrm{Th}} = i_{\mathrm{s}} Z_{\mathrm{Th}} \tag{3}$$

$$Z_{\mathrm{Th}} = R_{\mathrm{Th}} + \chi_{\mathrm{Th}} j \tag{4}$$

where i_{s} is the source current, R_{Th} and χ_{Th} are the Thévenin equivalent resistance and reactance, respectively. Accordingly, the optimal output impedance for the maximum power transfer can be calculated as,

$$R_{\mathrm{load}} = R_{\mathrm{Th}} = \frac{R_{\mathrm{s}}}{1 + R_{\mathrm{s}}^2 \left(\omega C_{\mathrm{s}} - \dfrac{1}{\omega L_{\mathrm{s}}} \right)^2} \tag{5.1}$$

$$\chi_{\text{load}} = -\chi_{\text{Th}} = \frac{-\left(\omega C_{\text{s}} - \dfrac{1}{\omega L_{\text{s}}}\right) R_{\text{s}}^2}{1 + R_{\text{s}}^2 \left(\omega C_{\text{s}} - \dfrac{1}{\omega L_{\text{s}}}\right)^2} \tag{5.2}$$

Eqs. (2) and (5) contain the frequency ω, implying the optimal impedance is only for the maximum output power with the known frequency of a harmonic input. In addition, Eqs. (2) and (5) assume a constant voltage or current source that is independent with the selected loading impedance. In vibration-based energy harvesting, however, random inputs (excitation sources) with a broad frequency bandwidth are very common. The circuit dynamics is coupled with structural dynamics. Therefore, the variation of the loading impedance in the circuit may affect the power input into the circuit, and the coupling effect of mechanical and electrical systems must be properly considered. In this regard, this classical IM theory provides an insufficient solution that cannot be directly applied to the optimization of vibration-based energy harvester. Therefore, an overall impedance optimization method is presented in the next section.

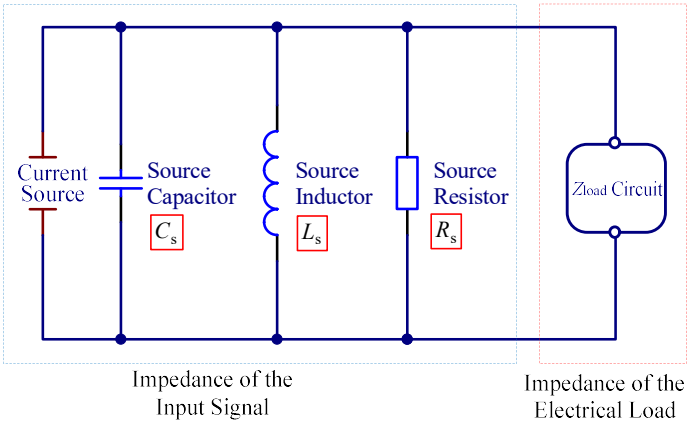

Fig. 2 Classical impedance matching with current source

3. Overall Impedance Optimization in SDOF Harvester

3.1 Structural and Electrical System

Fig. 3 shows a classical configuration of a vibration-based electromagnetic energy harvester, which comprises a SDOF primary structure and an electromagnetic transducer connected to a harvesting circuit. Herein, SDOF describes the dynamics of the mechanical structure. However, if the dynamics of the circuit is taken into account, the degrees of freedom of the whole system might be more than one.

The SDOF structure consists of a mass m_{str}, a stiffness k_{str} and an inherent damping c_{str}. The electromagnetic transducer typically consists of permanent magnets and coils that moves relative to each other, which could translate the structural oscillations into electricity generation. The coils inevitably own resistance R_{coil} and inductance features L_{coil}. Meanwhile, the electromagnetic transducer provides the parasitic damping c_p owing to various mechanical losses, such as friction and iron loss. As shown in Fig. 3, during the energy transformation, structural vibration generates an electromotive force (EMF) in the electromagnetic transducer, and the EMF further generates a current flowing through the attached harvesting circuit and internal impedance of transducer. In the meantime, an electromagnetic force proportional to the current would be generated and acting against the oscillation of the primary structure. Hence, the electromagnetic transducer contributes both the parasitic damping and electromagnetic forces to the mechanical structures, which may affect the structural vibrations as mentioned above.

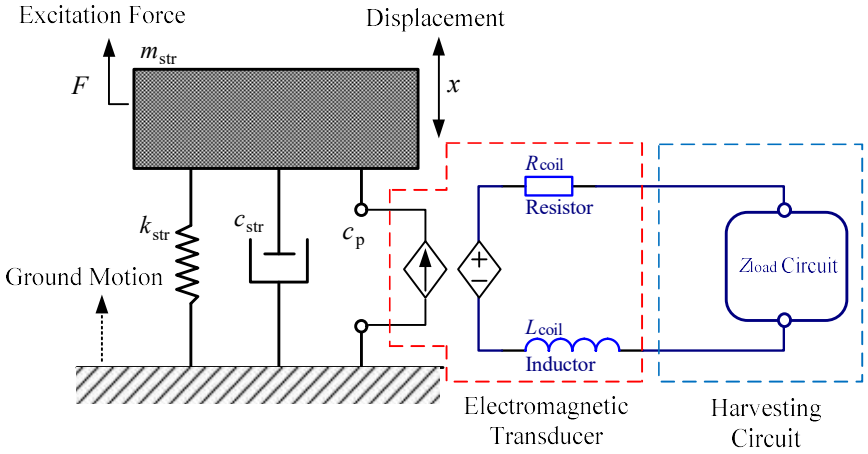

Fig. 3 SDOF structure with harvesting circuit

3.2 Equivalent Circuit Representation

Fig. 3 shows a coupled electro-mechanical system. Based on the analogy between electrical component and mechanical structures (Firestone, 1933; Zhu et al., 2013; Li and Zhu, 2018),

$$i = \frac{F}{K_{eq}^2} \tag{6.1}$$

$$V = K_{eq}^2 \dot{x} \tag{6.2}$$

$$L_{\mathrm{str}} = \frac{K_{\mathrm{eq}}^2}{k_{\mathrm{str}}} \tag{6.3}$$

$$C_{\mathrm{str}} = \frac{m_{\mathrm{str}}}{K_{\mathrm{eq}}^2} \tag{6.4}$$

$$R_{\mathrm{p}} = \frac{K_{\mathrm{eq}}^2}{c_{\mathrm{p}}}, \quad R_{\mathrm{str}} = \frac{K_{\mathrm{eq}}^2}{c_{\mathrm{str}}} \tag{6.5}$$

where F denotes the excitation force, $\dot{x}$ is the relative velocity between two terminals, and K_{eq} is the machine constant of electromagnetic device, L_{str}, C_{str} and R_{str} are structural equivalent inductance, capacitance and resistance, respectively, and R_{p} represents the equivalent resistance corresponding to parasitic damping. Then the coupled system shown in Fig. 3 could be represented by an alternative equivalent circuit (as shown in Fig. 4) that is entirely in the electrical domain. In this dynamic analogy, the dynamic force on the SDOF structure corresponds to an electrical current generator, and the vibration velocity corresponds to the voltage across the electrical elements. Notably, this topology is also applicable to the energy harvester subjected to a ground motion. In Fig. 4, the left blue block represents the equivalent part of the mechanical structure; and the red block represents the electromagnetic transducer. In this equivalent circuit, most of the electrical elements are connected in parallel with each other.

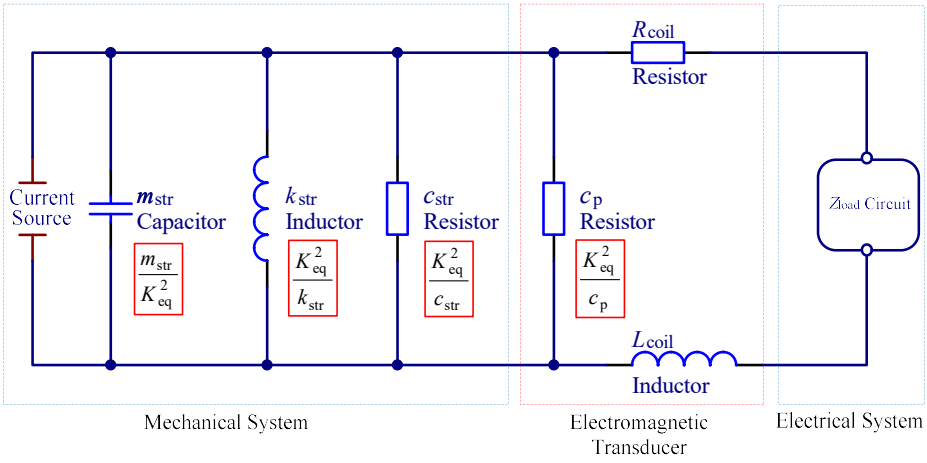

Fig. 4 Equivalent circuit for SDOF coupling system

3.3 Weakly Coupled System

In some cases with very small K_{eq} and c_{p}, the electromagnetic transducer produces small forces and thus the influence of the electromagnetic transducer connected to the energy

harvesting circuit on the overall dynamics is nearly negligible. Consequently, the whole system becomes weakly coupled, i.e., the input voltage to the electromagnetic transducer is mainly determined by the mechanical dynamics of the SDOF structure and remains nearly constant if the major mechanical and excitation parameters are fixed. In this case, the equivalent circuit can be simplified as Fig. 5 with an independent voltage source input to the electromagnetic transducer.

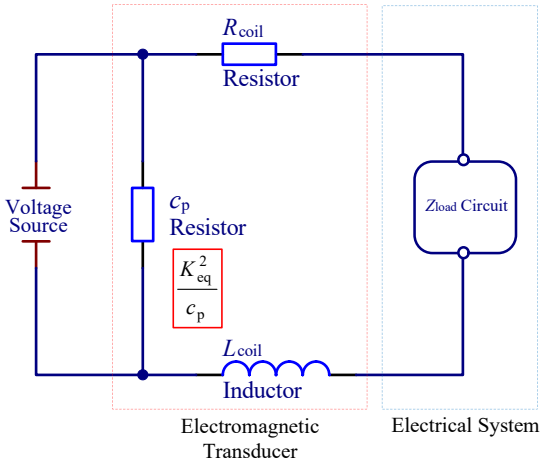

Fig. 5 Equivalent circuit for weakly coupled system

If the voltage source represents a harmonic input, the optimal impedance for the maximum output power can be easily obtained through the aforementioned Thévenin equivalent circuit analysis,

$$R_{\text{load}} = R_{\text{Th}} = R_{\text{coil}} \tag{7.1}$$

$$\chi_{\text{load}} = -\chi_{\text{Th}} = -\omega L_{\text{coil}} \tag{7.2}$$

This condition is consistent with the result in Eq. (2) for the classical IM, which demonstrates that the classical IM is applicable to the case of weakly coupled system. This conclusion is also extended to the weakly coupled MDOF energy harvester later on.

However, the above IM does not correspond to the optimal power efficiency in the circuit shown in Fig. 5. The optimal power efficiency condition will be discussed in detail in Subsection 3.4.2, which will be different from the IM condition. It is also noteworthy that Eq. (7) is only suitable for the optimal output power with a harmonic input/excitation. If the voltage source is replaced by a constant power source in Fig. 5, the optimal power efficiency condition, instead of the IM condition, will lead to the maximum output power. This conclusion will be relevant to the optimization under random excitation in the following section.

3.4 Strongly Coupled System

3.4.1 Overall IM under Harmonic Excitation

Given a strong electro-mechanical coupling system, the SDOF energy harvester can be described by the equivalent circuit shown in Fig. 4. Given a harmonic excitation (a harmonic force or ground motion), i.e. a harmonic current source with a frequency ω, the Thévenin equivalent impedance can be obtained by analyzing the circuit topology in Fig. 4:

$$\begin{aligned} Z_{\mathrm{Th}} &= \frac{1}{\frac{1}{R_{\mathrm{str}}}+\frac{1}{R_{\mathrm{p}}}+\omega C_{\mathrm{str}} j-\frac{j}{\omega L_{\mathrm{str}}}}+R_{\mathrm{coil}}+\omega L_{\mathrm{coil}} j \\ &= R_{\mathrm{Th}}+\chi_{\mathrm{Th}} j \end{aligned} \tag{8}$$

If the entire energy harvesting system is treated as a single circuit, the maximum output power under a harmonic excitation can be obtained by applying the overall IM. The optimal loading impedance should be the complex conjugate of the Thévenin equivalent impedance:

$$\begin{aligned} R_{\mathrm{load}} = R_{\mathrm{Th}} &= \frac{R_{\mathrm{p+str}}}{1+R_{\mathrm{p+str}}^2\left(\omega C_{\mathrm{str}}-1/\omega L_{\mathrm{str}}\right)^2}+R_{\mathrm{coil}} && \text{Electrical Domain} \\ &= \frac{\omega^2 K_{\mathrm{eq}}^2\left(c_{\mathrm{str}}+c_{\mathrm{cp}}\right)}{\omega^2\left(c_{\mathrm{str}}+c_{\mathrm{p}}\right)^2+\left(\omega^2 m_{\mathrm{str}}-k_{\mathrm{str}}\right)^2}+R_{\mathrm{coil}} && \text{Mechanical Domain} \end{aligned} \tag{9.1}$$

$$\begin{aligned} \chi_{\mathrm{load}} = -\chi_{\mathrm{Th}} &= \frac{-R_{\mathrm{p+str}}^2\left(1/\omega L_{\mathrm{str}}-\omega C_{\mathrm{str}}\right)}{1+R_{\mathrm{p+str}}^2\left(\omega C_{\mathrm{str}}-1/\omega L_{\mathrm{str}}\right)^2}-\omega L_{\mathrm{coil}} && \text{Electrical Domain} \\ &= \frac{-\omega K_{\mathrm{eq}}^2\left(k_{\mathrm{str}}-\omega^2 m_{\mathrm{str}}\right)}{\omega^2\left(c_{\mathrm{str}}+c_{\mathrm{p}}\right)^2+\left(\omega^2 m_{\mathrm{str}}-k_{\mathrm{str}}\right)^2}-\omega L_{\mathrm{coil}} && \text{Mechanical Domain} \end{aligned} \tag{9.2}$$

where $R_{\mathrm{p+str}}=\dfrac{R_{\mathrm{p}} R_{\mathrm{str}}}{R_{\mathrm{p}}+R_{\mathrm{str}}}$ is the total resistance considering R_{p} and R_{str} in parallel connection. This optimal condition, which is excitation frequency dependent, is actually consistent with the conclusions reported by Cheng et al. (2007) and Cammarano et al. (2010) who derived in electric and mechanical domains, respectively.

Eq. (9) indicates that the optimal loading impedance in the strongly coupled system depends not only on the transducer characteristics (i.e., R_{p}, R_{coil} and L_{coil}), but also on the structural characteristics, such as the equivalent resistor R_{str}, capacitor C_{str} and inductor L_{str}. The result theoretically demonstrates that the impedance optimization of electromagnetic

energy harvester should take the structural mechanical characteristics into consideration. With the consideration of the overall (mechanical and structural) impedance, the classical IM method can be extended to the optimization of energy harvesting circuit in the vibration-based electromagnetic energy harvester.

For an ideal case in which the primary structure is designed in resonance with the harmonic excitation with a frequency ω,

$$k_{\text{str}} = m_{\text{str}}\omega^2 \tag{10.1}$$

$$\omega L_{\text{str}} = \frac{1}{\omega C_{\text{str}}} \tag{10.2}$$

the optimal condition shown in Eq. (9) can be simplified as,

$$R_{\text{load}} = R_{\text{str+p}} + R_{\text{coil}} \tag{11.1}$$

$$\chi_{\text{load}} = -\omega L_{\text{coil}} \tag{11.2}$$

If the coil inductance is negligible, Eq. (11.1) provides the result consistent with that previously reported by Stephen (2006) for a resonant state.

The energy harvester in a resonant state certainly presents an ideal situation that maximizes the output power; while Eq. (9) presents a more general case in which the harmonic excitation frequency may deviate from the designed frequency of the energy harvester.

3.4.2 Power Efficiency

In the energy conversion process, various power losses and consumptions occur inevitably when the power flows through the whole system. Only a portion of the vibration power can be harvested. The power efficiency also is one index of common interest in energy harvesting performance evaluation. Zhu et al. (2012) and Shen et al. (2016) presents the overall power efficiency as the products of several sub-efficiencies,

$$P_{\text{out}} = P_{\text{in}} \cdot \eta = P_{\text{in}} \cdot \eta_1 \cdot \eta_2 \cdot \eta_3 \tag{12}$$

where P_{out} is the average output power from the energy harvester, P_{in} is the average input power to the whole system, η is the overall power efficiency in the whole system, η_1 denotes the ratio of the power in the branch with R_{coil} and Z_{load} to the total power consumption of the equivalent circuit, η_2 is the ratio of the output power on the loading resistance R_{load} to the

power consumed by this branch, and η_3 represents the power conversion ratio of the energy harvesting circuit. In practice, various types of circuits have been proposed to realize energy harvesting and synthetic impedance functions, such as H-bridge and buck-boost converter (Mitcheson et al. 2012; Shen et al. 2016). The design of these circuit topologies is beyond the scope of this study. For simplicity, the power consumption by the loading resistance R_{load} is considered as the output power in this study, η_3 is equal to one and will not be discussed. It also noteworthy that all the power items in this paper are average power unless otherwise stated.

Considering the equivalent circuit shown in Fig. 4, the ideal capacitor or inductor elements do not consume any power in a cycle, and only the resistors in the circuit are energy consuming or dissipating elements. Thus, the other two sub-efficiencies can be expressed as,

$$\eta_1 = \frac{R_{\text{p+str}} \cos^2 \theta}{R_{\text{load}} + R_{\text{coil}} + R_{\text{p+str}} \cos^2 \theta} \tag{13.1}$$

$$\eta_2 = \frac{R_{\text{load}}}{R_{\text{load}} + R_{\text{coil}}} \tag{13.2}$$

And the corresponding overall power efficiency is

$$\eta = \frac{R_{\text{p+str}} \cos^2 \theta}{R_{\text{load}} + R_{\text{coil}} + R_{\text{p+str}} \cos^2 \theta} \cdot \frac{R_{\text{load}}}{R_{\text{load}} + R_{\text{coil}}} \tag{14}$$

where θ stands for the phase angle between the current and voltage in the branch containing R_{coil}, L_{coil} and Z_{load}, as shown in Fig. 6.

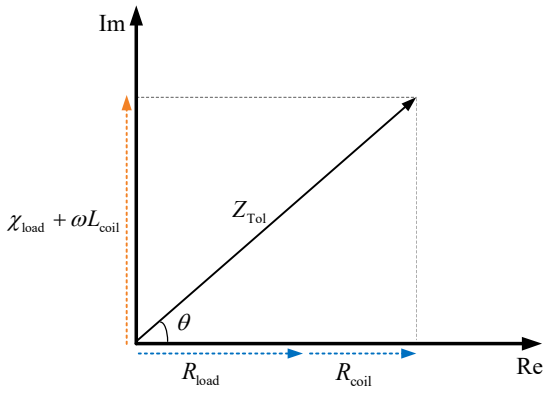

Fig. 6 Impedance vector diagram for transducer and harvesting circuit

If

$$\chi_{\text{load}} = -\omega L_{\text{coil}} \text{ (i.e. } \cos\theta = 1) \tag{15.1}$$

$$R_{\text{load}} = \sqrt{R_{\text{coil}}^2 + R_{\text{coil}} R_{\text{p+str}}} \tag{15.2}$$

the optimal power efficiency can be achieved,

$$\eta_{\text{opt}} = \frac{\sqrt{R_{\text{coil}}^2 + R_{\text{coil}} R_{\text{p+str}}}\, R_{\text{p+str}}}{R_{\text{p+str}} \left(\sqrt{R_{\text{coil}}^2 + R_{\text{coil}} R_{\text{p+str}}} + R_{\text{coil}} \right) + \left(\sqrt{R_{\text{coil}}^2 + R_{\text{coil}} R_{\text{p+str}}} + R_{\text{coil}} \right)^2} \tag{16}$$

Inspection of Eq. (15) demonstrates the optimal power efficiency requires the loading reactance to be the opposite number of the transducer's reactance. Eqs. (9) and (15) indicate that the optimal impedance values for the maximum output power and power efficiency are obviously different under a harmonic excitation. The explanation is that the input power P_{in} under a harmonic excitation varies with the electrical load. Consequently, the maximum power efficiency does not lead to the maximum output power.

Notably, given a small coil inductance of the electromagnetic transducer and low-frequency excitation, the reactance shown in Eq. (15.1) will be nearly negligible, and thus a pure resistive load can be used to optimize the efficiency. In this situation, only Eq. (15.2) needs to be adopted to obtain the optimal efficiency shown in Eq. (16).

In addition, Eqs. (15) and (16) do not depend on structural characteristics (such as m_{str} and k_{str}) other than structural inherent damping (c_{str} or R_{str}). Therefore, in the optimal power efficiency, the mechanical and electrical systems are coupled through the equivalent resistance R_{str} only. In real applications, we always try to minimize the inherent damping of the energy harvesting structures to enhance the efficiency. If the structural inherent damping becomes negligible ($c_{\text{str}} << c_{\text{p}}$), the equivalent resistance R_{str} becomes extremely large and the system becomes decoupled in terms of power efficiency. Consequently, the optimal conditions in Eq. (15) can be simplified as

$$\chi_{\text{load}} = -\omega L_{\text{coil}} \tag{17.1}$$

$$R_{\text{load}} = \sqrt{R_{\text{coil}}^2 + R_{\text{coil}} R_{\text{p}}} \tag{17.2}$$

for the weakly-coupled system. This result is identical to that derived by Zhu et al. (2012) who did taken into account any coupling effect.

3.4.3 Impedance Optimization under Random Excitation

Since AC power sources typically have a fixed frequency, random power sources rarely appear in the power electronics discussions. However, random excitations are common in vibration-based energy harvesters. By replacing the harmonic current source in Fig. 4 with a white noise random source, Eqs. (9) and (11) are no longer applicable because of the undetermined excitation frequency. Accordingly, the optimization of vibration-based energy harvesters under random excitations has received rare attention.

Shen et al. (2018) analyzed the stochastic vibrations of an SDOF energy harvester, in which the electromagnetic transducer is represented by a damping element. Their power spectrum density (PSD) analysis can give the input power with a resistive load as,

$$P_{\text{in}} = \begin{cases} \pi m_{\text{str}} S_0 & \text{if random gound motion} \\ \pi S_0 / m_{\text{str}} & \text{if random force excitation} \end{cases} \tag{18}$$

where S_0 represents the PSD of the random ground motion or force excitation. If the equivalent circuit in Fig. 4 is considered, the input power of open circuit can be expressed as

$$P_{\text{in}} = \pi S_{\text{I}} / C_{\text{str}} \tag{19}$$

where the average input power only depends on the PSD of the random current source S_{I} and the structural equivalent capacitor C_{str} in the circuit.

Considering the broadband characteristic of excitations, a pure resistive energy harvesting circuit is preferable in case of random excitations. Although the variation of the loading resistance may change the overall damping of the system, Eq. (19) shows that the input power remains constant under white noise excitations. The constant input power implies that the maximum output power and maximum power efficiency can be achieved simultaneously according to Eq. (12), which is different from the conclusion in the harmonic excitation case. Given a negligible coil inductance of the electromagnetic transducer, Eq. (15.2) provides a satisfactory solution to achieve the maximum output power and power efficiency under random excitations, where the power efficiency is described by Eq. (16).

A pure resistive energy harvesting circuit is assumed in the above discussion considering adding reactance to the output circuit may lower the power efficiency or even input power.

4. Overall Impedance Optimization in MDOF Harvester

4.1 MDOF Harvester

To expand the frequency bandwidth of energy harvesters, a number of MDOF energy harvesters with different structures have been proposed recently. For example, Tang and Zuo (2011) proposed to use dual-mass systems to enhance electromagnetic vibration energy harvesting performance. Xiao et al. (2016) proposed an improved MDOF harvester by introducing piezoelectric elements between every two oscillators. However, rare attention has been paid to the optimization of electrical load in these MDOF energy harvesters, especially when subjected to a random input. This subsection introduces the impedance optimization in a general MDOF energy harvester under harmonic and random excitations.

An MDOF harvester can be similarly represented by an equivalent electrical circuit, as shown in Fig. 7. Given a ground motion excitation, either harmonic or random, the current sources 1 to N are in phase and proportional; while under force excitations, these current sources may have different frequencies and magnitudes, if the external forces on each mass are independent.

If the structural inherent damping is negligible compared with the damping contributed by the electromagnetic transducer, all the equivalent resistors $R_{\mathrm{str\_i}}\left(\mathrm{i}=1,\cdots,\mathrm{N}\right)$ can be removed. In this situation, the Thévenin equivalent impedance can be calculated as follows,

$$Z_{\mathrm{Th}}=\frac{1}{\dfrac{1}{Z_{\mathrm{str\_2}}}+\dfrac{1}{R_{\mathrm{p}}}+\omega C_{\mathrm{str\_1}}j-\dfrac{j}{\omega L_{\mathrm{str\_1}}}}+R_{\mathrm{coil}}+\omega L_{\mathrm{coil}}j \tag{20}$$

where the form $Z_{\mathrm{str\_i}}$ can be obtained as

$$Z_{\mathrm{str\_i}}=\begin{cases}\dfrac{1}{1/Z_{\mathrm{str\_i+1}}+\omega C_{\mathrm{str\_i}}j}+\omega L_{\mathrm{str\_i}}j & \left(\mathrm{i}=2,3,\cdots,\mathrm{N}-1\right)\\ -j/\omega C_{\mathrm{str\_N}}+\omega L_{\mathrm{str\_N}}j & \left(\mathrm{i}=\mathrm{N}\right)\end{cases} \tag{21}$$

Then the optimal output impedance can be calculated directly as the complex conjugate of Z_{Th}. Notably, this optimal IM for output power is frequency-dependent, and is only suitable for a harmonic excitation. In a resonant state (i.e., the excitation frequency is equal to the natural

frequency), the optimal IM for the MDOF harvester becomes identical to that of SDOF scenario, i.e., Eq. (11).

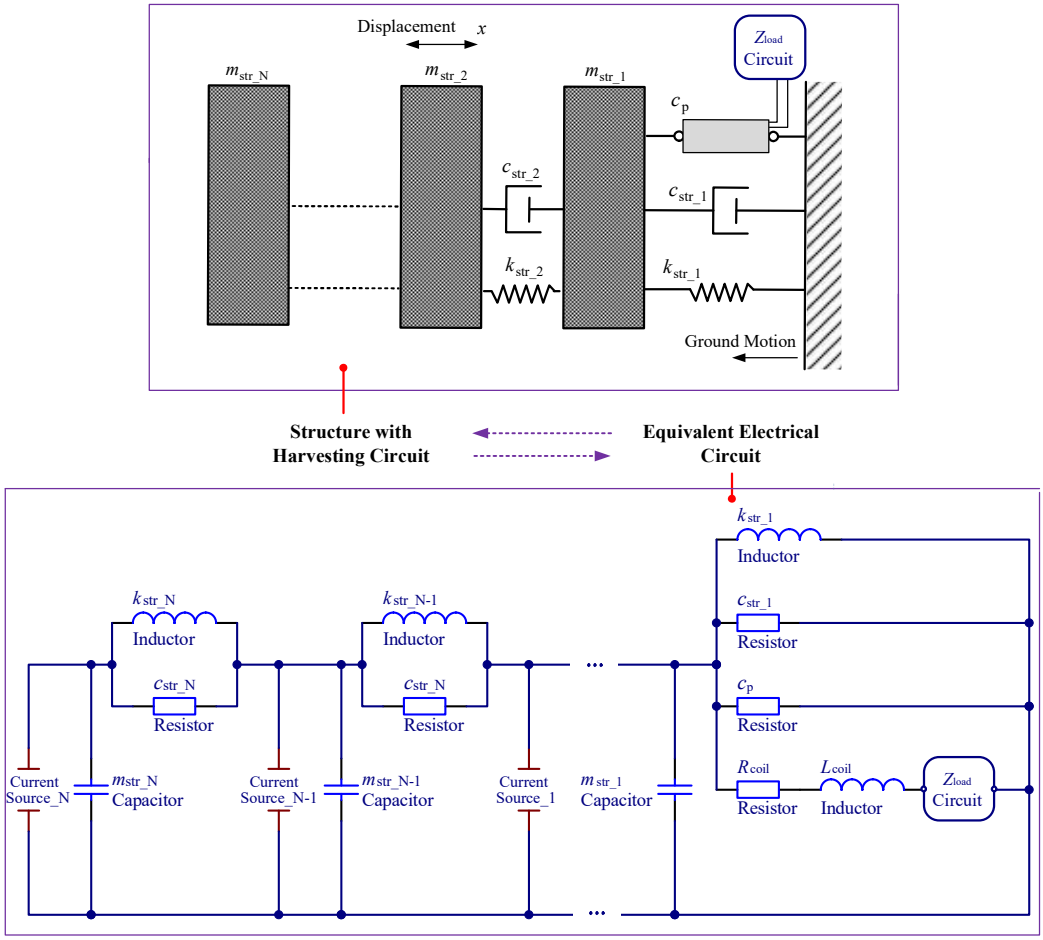

Fig. 7 MDOF energy harvester and the corresponding equivalent circuit

Similar to the SDOF case, a pure resistive output circuit is preferred for the MDOF energy harvester under a random excitation. Given the fixed structural characteristics and PSD of random input, the input power to the MDOF harvester under a white noise excitation is nearly constant (Shen et al. 2018) and independent with the change of the loading resistance. Considering the constant input power, the maximum output power will be consistent with the maximum power efficiency. In case that both the structural inherent damping and coil inductance are minimal, Eq. (17.2) introduced in Subsection. 3.4.3 can be still applied to the MDOF energy harvester to obtain the optimal impedance. Notably, a low structural inherent damping is highly desirable in vibration-based energy harvesters to achieve a satisfactory energy conversion ratio. Otherwise, a high structural inherent damping ratio will dissipate the

majority of the input power and lead to trivial output power. The effect of the inherent damping will be briefly discussed in the next section.

4.2. Summary of Overall Impedance Optimization of SDOF and MDOF harvester

The optimal impedance for the maximum output power was theoretically derived in this section in consideration of different types of excitations (harmonic and random). Table 1 summarizes the optimal electrical load that maximizes the output power in different scenarios and the corresponding assumptions.

Table 1. Optimal conditions for the output power in different scenarios.

Structural Type	Excitation	Load Impedance
SDOF/MDOF (weak coupling)	Harmonic	Eq. (7)
	Random[1]	Eq. (17.2)
SDOF (strong coupling)	Harmonic	Eq. (9)
	Random[1]	Eq. (15.2)
MDOF (strong coupling)	Harmonic	Eq. (20)
	Random[2]	Eq. (17.2)

Notes: 1. It assumes that the coil inductance is negligible; 2 It assumes that the coil inductance and structural inherent damping are negligible

5. Numerical Validation

5.1 Simulink Model

This section introduces the dynamic simulations of SDOF and 2DOF energy harvesters individually. Fig. 8 shows the simulation model of the SDOF harvester established in the Matlab/Simulink environment. The time step is set as 10^{-4} s to guarantee accurate circuit signals. The electromagnetic transducer is modelled by employing the measured parameters of a real linear-motion electromagnetic device (Moticont, model No. GVCM-095-051-01): machine constant $K_{\text{eq}} = 38\,\text{N/A}$, parasitic damping coefficient $c_{\text{p}} = 32.4\,\text{Ns/m}$, coil resistance $R_{\text{coil}} = 9.3\,\Omega$, and coil inductance $L_{\text{coil}} = 5\,\text{mH}$. The influence of such a small coil inductance is often negligible in low-frequency vibrations. In the numerical simulations of this study, the coil inductance is ignored unless otherwise stated. Two different types of ground motions, namely, harmonic and random ground motions, are applied to the concerned energy harvesters separately. The inherent damping of the structure is ignored.

The 2DOF energy harvester is simulated in a similar way. Table 2 lists the main parameters of the numerical models and excitations for both the SDOF and 2DOF energy harvesters. The mass and stiffness are determined to be compatible with the selected machine constant. Case 1 and Case 2 represent the resonant and non-resonant cases of the SDOF energy harvester; Case 4 and Case 5 represent the resonant and non-resonant cases of the MDOF energy harvester, where the resonant case corresponds to the second frequency; Case 3 and Case 6 represent white noise excitations with sufficiently broad bands of frequencies.

Table 2. Main parameters of the harvesters and excitation

Structural Types		Parameters	Value
SDOF	Structural parameters	Structural mass of, m_{str}	3 kg
		Structural stiffness of, k_{str}	10^3 N/m
		Natural frequency of, f_{res}	2.91 Hz
	Excitation cases	Case 1, Harmonica, f_{ex}	2.91 Hz
		Case 2, Harmonica, f_{ex}	2.50 Hz
		Case 3, Random, f_{ex}	0-500 Hz
2DOF	Structural parameters	Structural mass, m_{str_2}	0.8 kg
		Structural stiffness, k_{str_2}	300 N/m
		Structural mass, m_{str_1}	8 kg
		Structural stiffness, k_{str_1}	3 kN/m
		1st order resonant frequency, f_{res_1}	2.63 Hz
		2nd order resonant frequency, f_{res_2}	3.61 Hz
	Excitation cases	Case 4, Harmonica, f_{ex}	3.61 Hz
		Case 5, Harmonica, f_{ex}	3.50 Hz
		Case 6, Random, f_{ex}	0-500 Hz

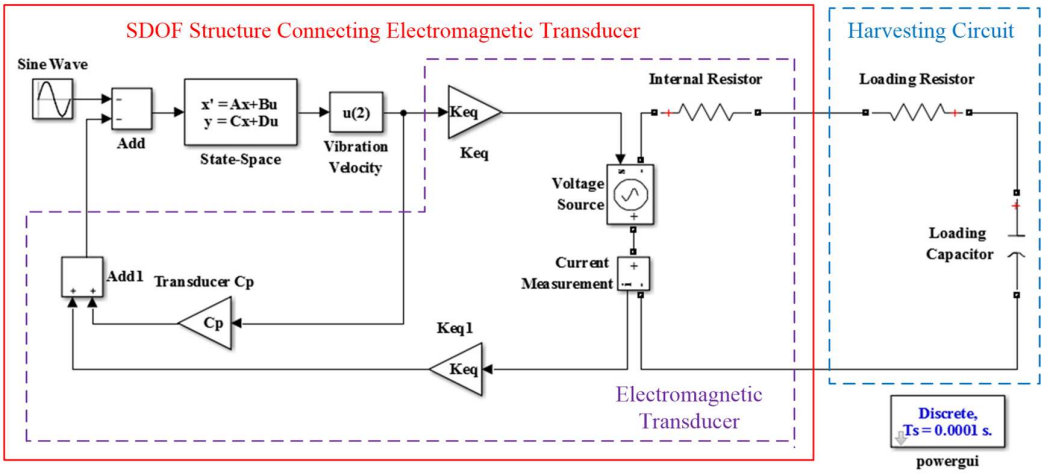

Fig. 8 Simulink model for the SDOF harvester

5.2 Optimal Impedance Results

Fig. 9 shows the variations of the optimal loading resistance R_{load} and reactance χ_{load} according to the overall IM (i.e., Eqs. (9) and (20), respectively) for the maximum output power under harmonic excitations. The optimal values of the two parameters (R_{load} and χ_{load}) are functions of the excitation frequency. In Fig. 9(a), the curve shapes of the resistance and reactance are symmetrical and anti-symmetrical, respectively. At the resonant frequency, the optimal resistance is maximum, while the optimal reactance is nearly zero. In Fig. 9(b), the number of peaks in optimal resistance is equal to the number of DOFs. In particular, for both the SDOF and MDOF cases, the varying optimal resistance has a lower bound of $R_{\text{coil}} = 9.3\Omega$, which is actually the result determined according to the classical IM without considering structural impedance (i.e., Eq. (2.1)). The required reactance is realized in the simplest way by connecting either an inductor or capacitor in the output circuit.

The frequencies corresponding to Cases 1, 2, 4, and 5 are also highlighted in Fig. 9. The corresponding optimal values for the output power can be read as follows:

$$\text{Case 1, Eq. (11): } R_{\text{load}} \approx 54\Omega,\ \chi_{\text{load}} \approx 0\Omega \tag{22.1}$$

$$\text{Case 2, Eq. (9): } R_{\text{load}} \approx 45\Omega,\ \chi_{\text{load}} \approx 18\Omega \tag{22.2}$$

$$\text{Case 4, Eq. (11): } R_{\text{load}} \approx 54\Omega,\ \chi_{\text{load}} \approx 0\Omega \tag{22.3}$$

$$\text{Case 5, Eq. (20): } R_{\text{load}} \approx 40\Omega,\ \chi_{\text{load}} \approx 20\Omega \tag{22.4}$$

Under random excitations (Cases 3 and 6), the optimal resistance is determined for the maximum efficiency as

$$\text{Optimal Efficiency, Eq. (15):}\ \ R_{\text{load}} \approx 22.4\Omega\,,\ \ \chi_{\text{load}} \approx 0\Omega \tag{23}$$

which is frequency independent.

Another case, the classical IM, is also considered for comparison in the following subsection:

$$\text{Classical IM:}\ \ R_{\text{load}} = R_{\text{coil}} = 9.3\Omega\,,\ \ \chi_{\text{load}} \approx 0\Omega \tag{24}$$

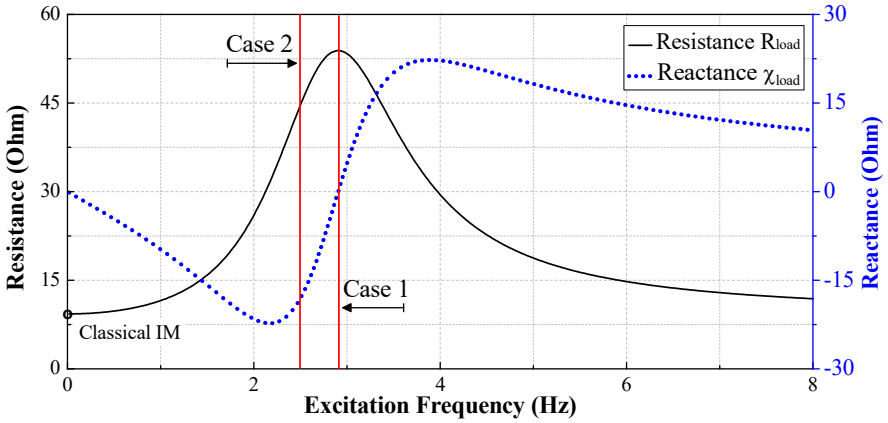

(a) SDOF energy harvester

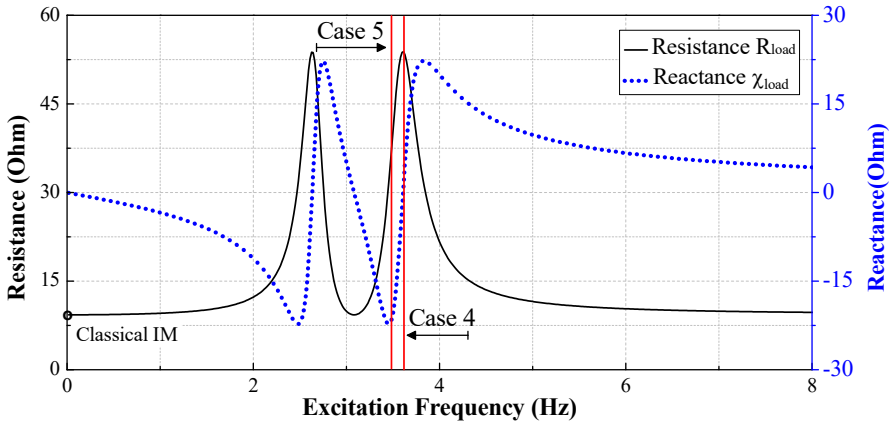

(b) 2DOF energy harvester

Fig. 9 IM results for harmonic excitation

5.3 Simulation Results of SDOF Harvesters

5.3.1 Case 1: Resonant SDOF Harvester

In Case 1, the SDOF energy harvester is subjected to a harmonic excitation frequency equal to the resonant frequency of the mechanical structure. Fig. 10(a) illustrates the variations of P_{in} and P_{out} with the loading resistance R_{load} in Case 1. The total input power P_{in} increases monotonically with the loading resistance, while the output power curve exhibits a peak value. It can be observed that the loading resistance $R_{load} = 54\Omega$ corresponds to the maximum output power $P_{max} = 28.7$ mW, which validates the theoretical prediction by Eq. (22.1). Compared with the result for the classical IM (as shown by the dashed line), the optimal output power of the overall IM is significantly enhanced by 100%. This comparison demonstrates that the impedance optimization in vibration-based energy harvesting has to take into account the primary structure and transducer, rather than implementing the classical IM directly.

Fig. 10(b) shows the variation of the power efficiency with the loading resistance. Apparently, the maximum power efficiency does not occur simultaneously with the maximum output power, owing to the varying input power. The maximum power efficiency occurs when the resistance $R_{load} = 22\Omega$, which accurately agrees with the theoretical predication by Eq. (23). The maximum power efficiency reaches only 41%, because the relatively large parasitic damping and coil resistance are considered in this numerical model.

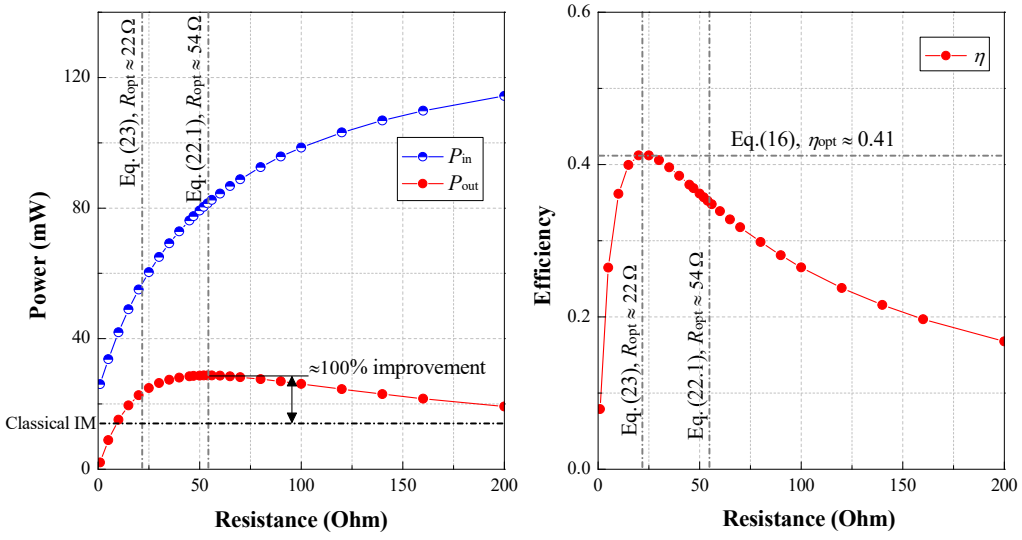

(a) Output power (b) Power efficiency

Fig. 10 Energy harvesting performance vs. R_{load} in a resonant state: SDOF harvester

5.3.2 Case 2: Non-resonant SDOF Harvester

In Case 2, the SDOF energy harvester is subjected to a harmonic frequency less than the structural resonant frequency. As mentioned in Subsection 4.2, the optimal impedance for output power can be predicted as $R_{\text{load}} = 45\Omega$ and $\chi_{\text{load}} = 18\Omega$ (C=3.5mF). Figs. 11-12 show the corresponding harvesting performance under the fixed optimal resistance or capacitance, respectively. The output power varies significantly with the increasing loading resistance, if the capacitance is fixed; however, after reaching its peak value, the output power is insensitive to the capacitance and only drops very slightly with the further increase in the capacitance. Such insensitivity is mainly due to the large parasitic damping and coil resistance considered for the electromagnetic transducer. The effect of the optimal capacitance will be more obvious if significantly smaller parasitic damping and coil resistance are adopted.

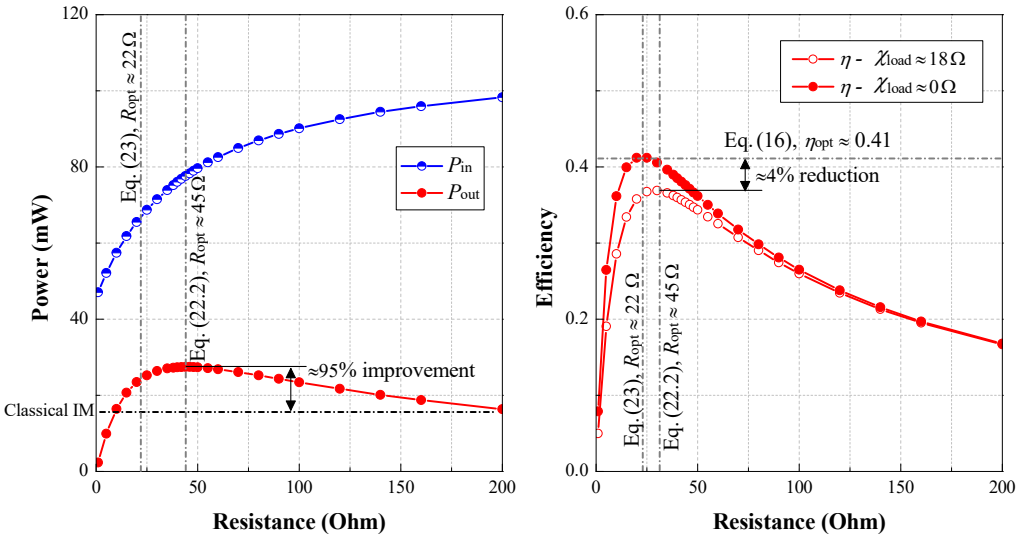

(a) Output power (b) Power efficiency

Fig. 11 Energy harvesting performance vs. R_{load} in a non-resonant state: SDOF harvester

With the adopted overall IM framework, the optimal output power shown in Fig. 11(a) is enhanced by approximately 95%, compared with that with classical IM. Fig. 11(b) shows the variation of the power efficiency with the loading resistance R_{load}, wherein the loading reactance is equal to 18Ω and zero individually. Both the curves indicate that the optimal loading resistance for the maximum output power does not correspond to the maximum power efficiency. The existence of the reactance in the load slightly decreases the peak power

efficiency, and the maximum power efficiency (i.e., 41%) occurs in a pure resistive load circuit when $R_{load} = 45\Omega$, as predicted by Eq. (23).

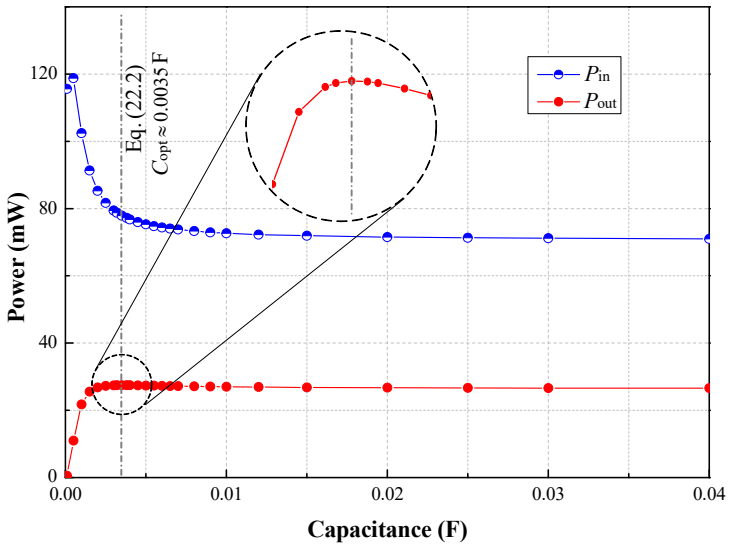

Fig. 12 Output power vs. C_{load} in a non-resonant state: SDOF harvester

5.3.3 Case 3: Randomly-excited SDOF Harvester

A pure loading resistance $R_{load} = 22\Omega$ is adopted when the SDOF energy harvester is subjected to a broadband random ground motion. Fig. 13 shows the PSD of the input ground acceleration, which represents a white noise input. This excitation bandwidth ranges from 0-500Hz with a constant PSD value of around 0.01 $(m/s^2)^2/Hz$.

Fig. 14 illustrates the output power and power efficiency variations with the loading resistance in Case 3. The total input power P_{in} keeps nearly constant as prediction and is independent with the change of the loading resistance. Consequently, the maximum output power and maximum power efficiency occur simultaneously when the loading resistance is $R_{load} = 22\Omega$, and the maximum power efficiency is 41%. These results accurately agree with the prediction in Subsection 4.2. Compared with the classical IM, the output power has a 17% improvement using the optimal loading resistance. This improvement demonstrates the benefit of using the proposed optimal impedance for power efficiency in the design of electromagnetic vibration-based energy harvesters under random excitations. The classical IM cannot provide an optimum solution for the output power and power efficiency.

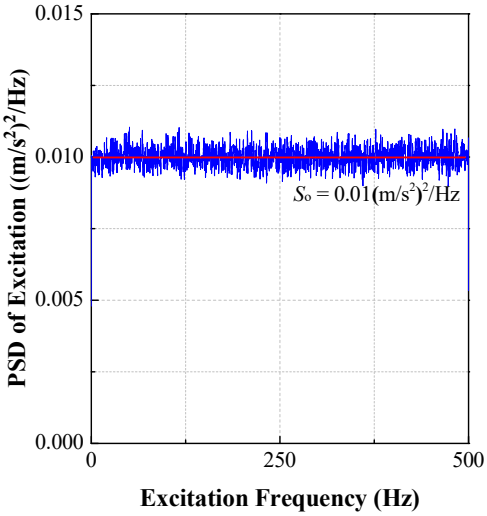

Fig. 13 PSD of the ground acceleration

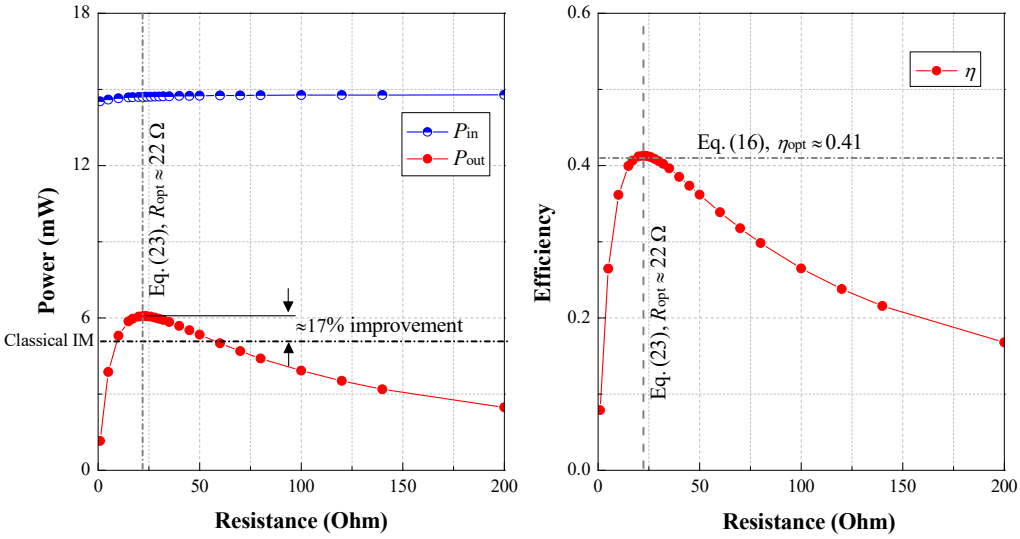

(a) Output power (b) Power efficiency

Fig. 14 Energy harvesting performance vs. R_{load} in random excitation: SDOF harvester

5.4 Simulation Results of 2DOF Harvester

This subsection presents the simulation results of the 2DOF energy harvester under different excitations. As the 2DOF structure represents a more general case compared with the SDOF one, more parametric analyses are also included in this subsection to examine the effects of different factors.

5.4.1 Cases 4-5: Harmonically-excited 2DOF Harvester

Case 4 presents the resonant case in which the 2DOF energy harvester is excited with a harmonic frequency equal to its 2nd order natural frequency. The optimal impedance for the output power and power efficiency are $54\,\Omega$ and $22\,\Omega$, respectively. The observations in the energy harvesting performance are similar to those reported in Case 1 and thus are not reported herein. The output power determined with the overall IM is nearly twice that with classical IM.

Case 5 presents the non-resonant case with the excitation frequency of 3.5Hz. The theoretical optimal impedance for the output power is $40\,\Omega$ and $2.2\,\text{mF}$, while the optimal impedance for the power efficiency is 22 Ω. The observations similar to those in Case 2 can be made, as shown in Fig. 15. The maximum output power and power efficiency do not occur simultaneously under harmonic excitations. Connecting a capacitor lowers the power efficiency compared with a pure resistor circuit.

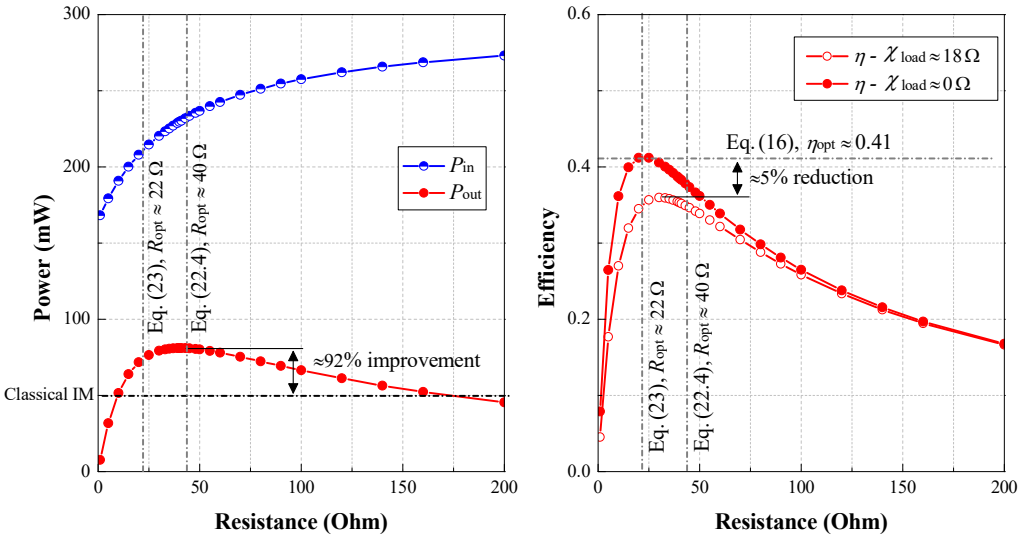

(a) Output power (b) Power efficiency

Fig. 15 Energy harvesting performance vs. R_{load} in a non-resonant state: 2DOF harvester

Cases 4 and 5 shows the energy harvesting performance for two individual frequencies. By applying the overall IM strategy to other harmonic frequencies of excitations, the energy harvesting performance over the frequency range can be obtained. Fig. 16 shows the frequency response function (FRF) of the normalized output power obtained through a series of simulations. The envelope corresponding to the classical IM is also illustrated for comparison. Compared with the classical IM, the overall IM strategy can significantly improve the output

power, especially near the resonant range, under harmonic excitations. This comparison demonstrates the importance of load impedance optimization in the performance of vibration-based energy harvesters.

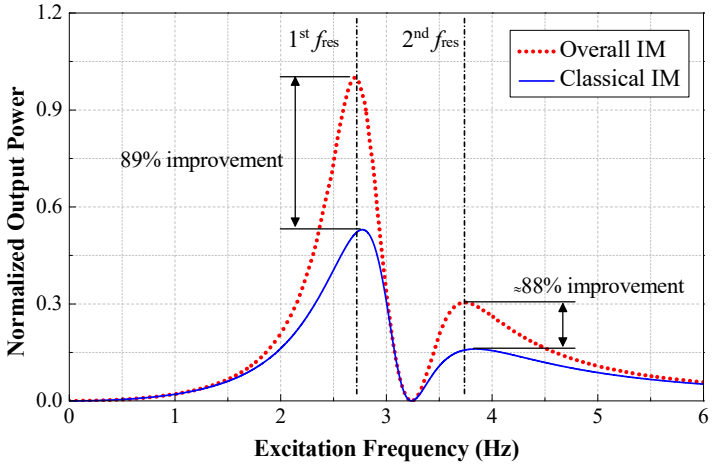

Fig. 16 Overall tuning performance: 2DOF harvester

5.4.2 Cases 6: Randomly-excited 2DOF Harvester

Under a random excitation, the optimal impedance values for the maximum output power and power efficiency are identical (i.e., Eq. (23)). Fig. 17 show the corresponding energy harvesting performance under a random ground motion, where the ground acceleration is the same as that described in Section 4.3.3. The variations of energy harvesting performance are similar to those of the SDOF harvester in Case 3. The optimal output power and power efficiency occur at the predicted locations. Compared with the classical IM, the power improvement is around 17%, demonstrating the effectiveness of the proposed optimal impedance for the MDOF energy harvester under random excitations.

Although the random ground motion is approximately white noise, the vibration of the 2DOF system is still dominated by the natural frequencies. Strictly speaking, the input to the electromagnetic transducer is a filtered signal that is no longer white noise. If the vibration is dominated by the natural frequencies, can we adopt the impedance setting for a resonant state in this random case? Fig. 18 compares the output power FRFs using two optimal impedance settings for resonance (i.e., Eq. (22.3)) and random excitation (i.e., Eq. (23)), respectively. It is not surprising to observe that the former produces higher power corresponding to the resonant peaks. However, when considering the area under the curves that represent the total output power under a random excitation, the optimal impedance defined in Eq. (23) leads to 13.6%

improvement in the total output power compared with Eq. (22.3.). This result demonstrates the need and benefit of adopting different optimal impedance setting for a random case, as proposed in this study, instead of optimal impedance setting for resonance.

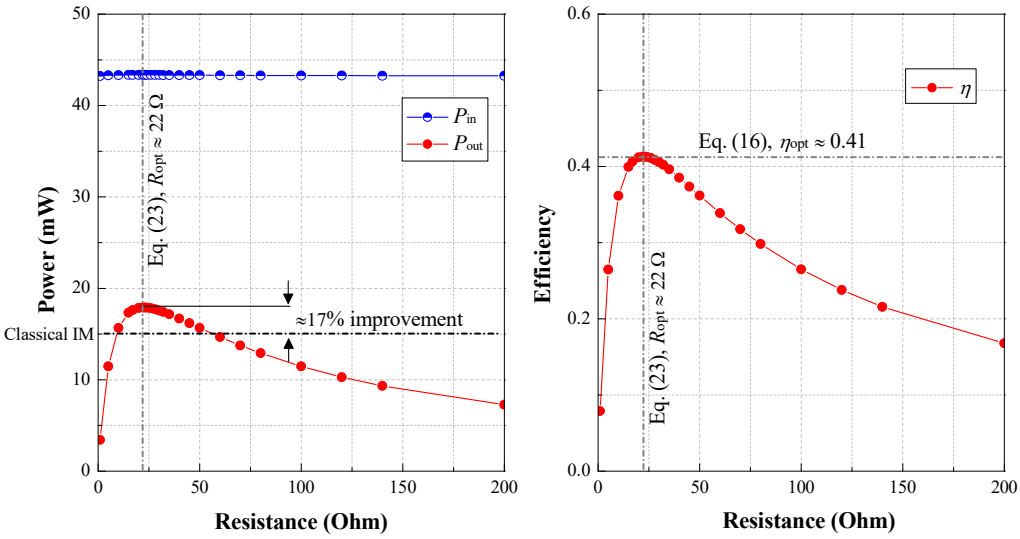

(a) Output power (b) Power efficiency

Fig. 17 Energy harvesting performance vs. R_{load} under random excitations: 2DOF harvester

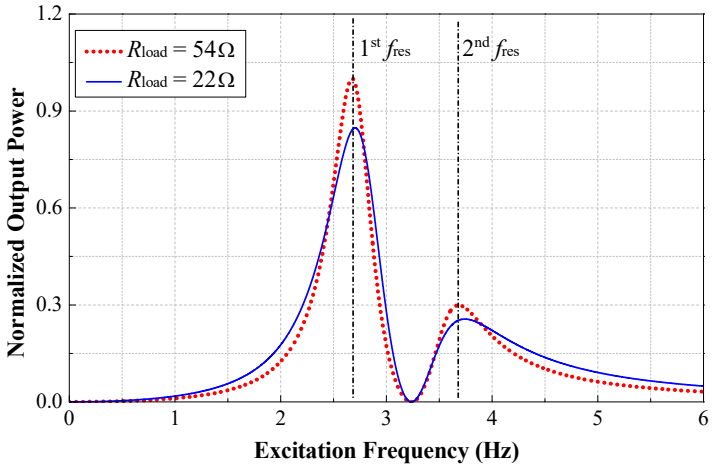

Fig. 18 Output power FRF comparison: 2DOF harvester

5.4.3 Effect of Structural Inherent Damping

Notably, the structural inherent damping is ignored in the aforementioned numerical case studies. This subsection examines the impact of structural inherent damping (i.e. R_{str}) on the optimal impedance and output power by taking Case 4 as an example.

In Case 4 for the second order resonance, the optimal impedance is shown in Eq. (22.3) if structural inherent damping is neglected. With the consideration of structural inherent damping, both the optimal impedance values and output power changes with the increasing damping ratio of the mechanical structure, as shown in Fig. 19. A large damping ratio leads to a large discrepancy in the output power shown in Fig. 19(b). However, the structural inherent ratio needs to be minimized in consideration of power efficiency in real applications. Given a low damping ratio (e.g., the 2nd order damping ratio $\zeta_{str\_2} < 4\%$), the difference in the output power is actually minimal (5% error). Similar results can be observed in the random excitation case. These observations justify that slight structural damping is typically ignorable in the aforementioned numerical simulations.

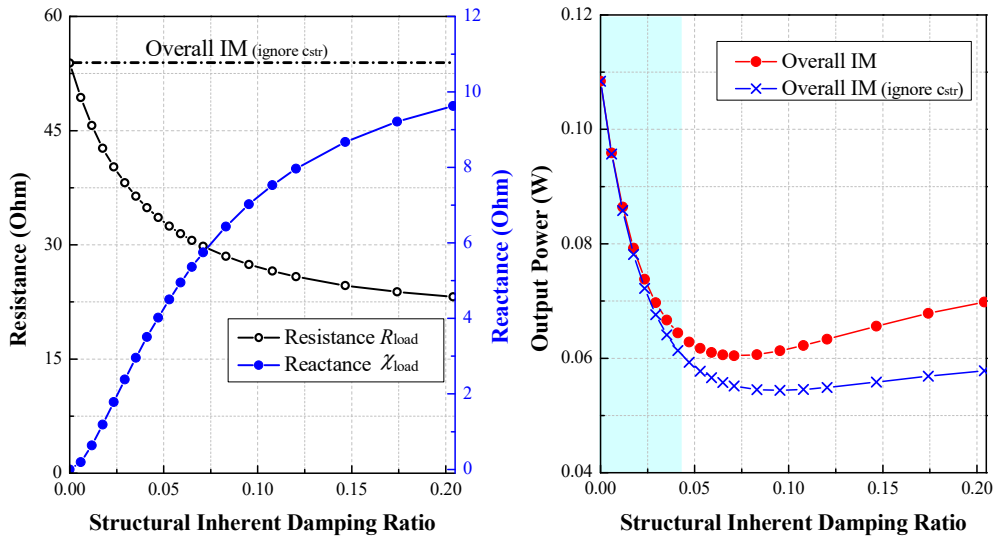

(a) Impedance (b) Output power

Fig. 19 Influence of inherent damping in harmonica excitation

6. Conclusions

This paper proposes a unified strategy for overall impedance optimization that considers structural and electrical dynamics in vibration-based electromagnetic energy harvesters. A

general equivalent circuit models for SDOF or MDOF harvesters were developed, and subsequently, the corresponding optimal impedance for the maximum output power and power efficiency was derived theoretically in consideration of different types of excitations (harmonic and random). Numerical case studies were conducted to validate the effectiveness and accuracy of the proposed overall impedance optimization. Based on the results of the theoretical derivation and numerical simulations, the following major conclusions can be drawn in this study:

(1) The classical IM in power electronics cannot guarantee a maximum output power in electromagnetic vibration-based energy harvesters with strong coupling effect between electric and mechanical systems.

(2) The dynamic analogy between mechanical and electrical systems enables to represent an SDOF or MDOF energy harvester using an equivalent circuit model. This equivalent representation provides a convenient and straightforward tool for the optimization of load impedance of energy harvesting circuit.

(3) Under harmonic excitations, the overall IM that considers the equivalent impedance of the primary structure and transducer can achieve the maximum output power in vibration-based energy harvesters. The corresponding optimal impedance values are thus frequency-dependent.

(4) Under harmonic excitations, the maximum output power does not correspond to the maximum power efficiency. The optimal solution for the maximum power efficiency is dependent on the structural inherent damping and transducer's parasitic damping. Incorporating reactance in the harvesting circuit may have a negative impact on the power efficiency, and thus a pure resistive circuit is preferable from the power efficiency perspective.

(5) Under random excitations, the maximum output power and power efficiency can be achieved simultaneously, given a relatively low damping level of the primary structure of an energy harvester. Therefore, the optimal impedance for the maximum power efficiency can be applied in a random excitation case. Such optimal impedance is frequency-independent if the coil inductance is negligible.

(6) If the inherent damping of an energy harvester structure is low, neglecting structural inherent damping in the overall impedance optimization has minimal impact on the energy harvesting performance under harmonica or random excitations.

It is noteworthy that the enhancement of energy harvesting performance can be realized by adjusting either electrical or mechanical systems. This study only focused on the optimization of the electric impedance of energy harvest circuits. However, given the equivalent conversion between the mechanical structures and electric circuits, the proposed methodology in this study will also shed light on the optimal design of mechanical parts.

Acknowledgment

The authors are grateful for the financial support provided by the Research Grants Council of Hong Kong through the Research Impact Fund (PolyU R5020-18), the NSFC/RGC Joint Research Scheme (N_PolyU533/17, 51761165022), and the Theme-based Research Scheme (T22-502/18-R). The findings and opinions expressed in this paper are from the authors alone and are unnecessarily the views of the sponsors.

References

Aldraihem O, Baz A. Energy harvester with a dynamic magnifier[J]. Journal of Intelligent Material Systems and Structures, 2011, 22(6): 521-530.

Cahill P, Nuallain N A N, Jackson N, et al. Energy harvesting from train-induced response in bridges[J]. Journal of Bridge Engineering, 2014, 19(9): 04014034.

Cammarano A, Burrow S G, Barton D A W, et al. Tuning a resonant energy harvester using a generalized electrical load[J]. Smart Materials and Structures, 2010, 19(5): 055003.

Cammarano A, Neild S A, Burrow S G, et al. Optimum resistive loads for vibration-based electromagnetic energy harvesters with a stiffening nonlinearity[J]. Journal of Intelligent Material Systems and Structures, 2014, 25(14): 1757-1770.

Challa V R, Prasad M G, Fisher F T. Towards an autonomous self-tuning vibration energy harvesting device for wireless sensor network applications[J]. Smart Materials and Structures, 2011, 20(2): 025004.

Cheng S, Wang N, Arnold D P. Modeling of magnetic vibrational energy harvesters using equivalent circuit representations[J]. Journal of Micromechanics and Microengineering, 2007, 17(11): 2328.

Erturk, A. (2009). Electromechanical modeling of piezoelectric energy harvesters (Doctoral dissertation, Virginia Tech).

Firestone F A. A new analogy between mechanical and electrical systems[J]. The Journal of the Acoustical Society of America, 1933, 4(3): 249-267.

Hambley A R, Kumar N, Kulkarni A R. Electrical engineering: principles and applications[M]. Upper Saddle River, NJ: Pearson Prentice Hall, 2008.

Iqbal M, Khan F U. Hybrid vibration and wind energy harvesting using combined piezoelectric and electromagnetic conversion for bridge health monitoring applications[J]. Energy conversion and management, 2018, 172: 611-618.

Kasyap A, Lim J, Johnson D, et al. Energy reclamation from a vibrating piezoceramic composite beam[C]//Proceedings of 9th International Congress on Sound and Vibration. 2002, 9(271): 36-43.

Kong N A, Ha D S, Erturk A, et al. Resistive impedance matching circuit for piezoelectric energy harvesting[J]. Journal of Intelligent Material Systems and Structures, 2010, 21(13): 1293-1302.

Li J, Zhu S. Versatile Behaviors of Electromagnetic Shunt Damper With Negative Impedance Converter[J]. IEEE/ASME Transactions on Mechatronics, 2018.

Liao Y, Sodano H. Optimal power, power limit and damping of vibration based piezoelectric power harvesters[J]. Smart Materials and Structures, 2018, 27(7): 075057.

Liu M, Tai W C, Zuo L. Toward broadband vibration energy harvesting via mechanical motion-rectification induced inertia nonlinearity[J]. Smart Materials and Structures, 2018, 27(7): 075022.

Magdy M M, El-Bab A M R F, Assal S F M. Design methodology of a micro-scale 2-DOF energy harvesting device for low frequency and wide bandwidth[J]. Journal of Sensor Technology, 2014, 4(02): 37.

Mitcheson P D. Analysis and optimisation of energy-harvesting micro-generator systems[D]. Imperial College London (University of London), 2005.

Mitcheson P D, Toh T T, Wong K H, et al. Tuning the resonant frequency and damping of an electromagnetic energy harvester using power electronics[J]. IEEE Transactions on Circuits and Systems II: Express Briefs, 2011, 58(12): 792-796.

Park G, Rosing T, Todd M D, et al. Energy harvesting for structural health monitoring sensor networks[J]. Journal of Infrastructure Systems, 2008, 14(1): 64-79.

Priya S. Modeling of electric energy harvesting using piezoelectric windmill[J]. Applied Physics Letters, 2005, 87(18): 184101.

Saha C R, O'Donnell T, Loder H, et al. Optimization of an electromagnetic energy harvesting device[J]. IEEE Transactions on Magnetics, 2006, 42(10): 3509-3511.

Sazonov E, Li H, Curry D, Pillay P. Self-powered sensors for monitoring of highway bridges. IEEE Sens J 2009;9:1422–9.

Shen W. Electromagnetic damping and energy harvesting devices in civil structures[D]. The Hong Kong Polytechnic University, 2014.

Shen W, Zhu S, Xu Y. An experimental study on self-powered vibration control and monitoring system using electromagnetic TMD and wireless sensors[J]. Sensors and actuators A: physical, 2012, 180: 166-176.

Shen W, Zhu S, Zhu H. Experimental study on using electromagnetic devices on bridge stay cables for simultaneous energy harvesting and vibration damping[J]. Smart Materials and Structures, 2016, 25(6): 065011.

Shen W, Zhu S, Zhu H. Unify energy harvesting and vibration control functions in randomly excited structures with electromagnetic devices[J]. Journal of Engineering Mechanics, 2018, 145(1): 04018115.

Stephen N G. On energy harvesting from ambient vibration[J]. Journal of sound and vibration, 2006, 293(1): 409-425.

Tang L, Yang Y, Soh C K. Toward broadband vibration-based energy harvesting[J]. Journal of intelligent material systems and structures, 2010, 21(18): 1867-1897.

Tang L, Yang Y. A multiple-degree-of-freedom piezoelectric energy harvesting model[J]. Journal of Intelligent Material Systems and Structures, 2012, 23(14): 1631-1647.

Tang X, Zuo L. Enhanced vibration energy harvesting using dual-mass systems[J]. Journal of sound and vibration, 2011, 330(21): 5199-5209.

Williams C B, Shearwood C, Harradine M A, et al. Development of an electromagnetic micro-generator[J]. IEE Proceedings-Circuits, Devices and Systems, 2001, 148(6): 337-342.

Xiao H, Wang X, John S. A multi-degree of freedom piezoelectric vibration energy harvester with piezoelectric elements inserted between two nearby oscillators[J]. Mechanical Systems and Signal Processing, 2016, 68: 138-154.

Yang B, Lee C, Xiang W, et al. Electromagnetic energy harvesting from vibrations of multiple frequencies[J]. Journal of Micromechanics and Microengineering, 2009, 19(3): 035001.

Ye J, Lu Z, Chen C, et al. Power analysis of a single degree of freedom (DOF) vibration energy harvesting system considering controlled linear electric machines[C]//Transportation Electrification Conference and Expo (ITEC), 2017 IEEE. 2017: 158-163.

Zhao B, Liang J, Zhao K. Phase-Variable Control of Parallel Synchronized Triple Bias-Flips Interface Circuit towards Broadband Piezoelectric Energy Harvesting[C]//2018 IEEE International Symposium on Circuits and Systems (ISCAS). IEEE, 2018: 1-5.

Zhu S, Shen W, Qian X. Dynamic analogy between an electromagnetic shunt damper and a tuned mass damper[J]. Smart Materials and Structures, 2013, 22(11): 115018.

Zhu S, Shen W, Xu Y. Linear electromagnetic devices for vibration damping and energy harvesting: modeling and testing[J]. Engineering Structures, 2012, 34: 198-212.